Investigation of laser induced phosphorescence and fluorescence of acetone at low pressure for molecular tagging velocimetry in gas microflows

Hacene SI HADJ MOHAND[1,*], Feriel SAMOUDA[1] Christine BARROT[1], Stéphane COLIN[1] ,
Aldo FREZZOTTI[2],

* Corresponding author: Tel.: ++33 (0)561171110; Email: sihadjmo@insa-toulouse.fr
1 Université de Toulouse, Institut Clément Ader, Toulouse, France
2 Dipartimento di Scienze & Tecnologie Aerospaziali,Politecnico di Milano, Italy

Abstract Laser-induced fluorescence and phosphorescence properties of gaseous acetone in argon are measured and analyzed in a pressure ranging from 10^5 to 10^2 Pa, with the aim of analyzing by molecular tagging velocimetry gas microflows in rarefied regimes which requires operation at low pressure. Acetone is excited at a wavelength of 266 nm and immediately emits short lifetime fluorescence rapidly followed by long lifetime phosphorescence. At atmospheric pressure, the early phosphorescence intensity is more than 600 times lower than the fluorescence one. The phosphorescence signal is rapidly decreasing with time, closely following a power law. Both fluorescence and phosphorescence signals are decreasing with pressure. The systematic analysis of fluorescence and phosphorescence of acetone molecules shows that although the signal is dramatically reduced at low pressure, the on-chip integration technique and the optimization of the acquisition parameters provide an exploitable signal for molecular tagging velocimetry in rarefied microflows, in a Knudsen number range corresponding to the early slip flow regime.

Keywords: gas microflow, rarefied gas, molecular tagging velocimetry, fluorescence, phosphorescence, acetone, diffusion

1. Introduction

A number of microfluidic applications involve gas microflows in the slip flow regime (Zhang et al., 2012), characterized by a velocity slip and a temperature jump at the wall. Various models have been proposed in the literature (Colin, 2012; Zhang et al., 2012); however experimental datas mainly concern flowrate measurements (Morini et al., 2011). Local information on velocity fields is nevertheless necessary to improve the discussion on theoretical models for slip boundary conditions. The molecular tagging velocimetry (MTV) could be a well-suited technique, as it avoids using particles subjected to Brownian motion. MTV uses seeding gas molecules, such as acetone, which become luminescent once excited with a UV light. The region tagged by a UV laser is observed at two successive times – the first time can correspond to fluorescence signal and the second one to phosphorescence signal – and the velocity field is deduced from the displacement and deformation analysis of the tagged region (Koochesfahani, 1999). The spatial resolution, however, is constrained by the laser beam diameter, with a typical minimum value of the order of 30 µm, which requires operating in channels with a hydraulic diameter around 1 mm. For this reason, microflows in the slip flow regime should be analyzed with Knudsen similitude, reducing the pressure in order to reach Knudsen numbers in the range [10^{-3} – 10^{-1}], corresponding to this regime. Preliminary velocity profiles have previously been obtained at atmospheric pressure, i.e. in the continuum flow regime (Samouda et al., 2013). Applying the technique to rarefied gas flows requires a precise knowledge of acetone luminescence properties at low pressure, which is not documented in the literature.

The photo-physical process of acetone exci-

tation-deexcitation is illustrated in Fig. 1. Acetone molecules can be excited by photons within their absorption band (225–320 nm), leading to a transition of the molecules from a vibrational level of the ground electronic state S_0 to a vibrational level of the first excited singlet state S_1. These molecules can return to the initial state S_0 following either a non-radiative process, either fluorescent or phosphorescent radiative processes (Tran et al., 2006). The fraction of the molecules following one of these processes depends on the operating conditions and the species composition.

In the non-radiative process, which includes vibrational relaxation, internal conversion, and collisional quenching (mainly with O_2 molecules), no light is emitted by the molecules.

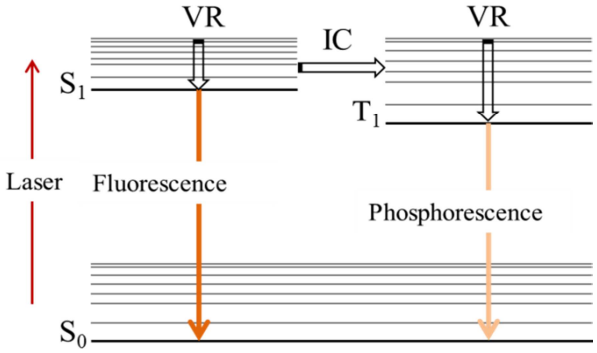

Fig. 1 Jablonski diagram illustrating a simplified model of acetone photo-physics. Adapted from (Charogiannis and Beyrau, 2013).

In the radiative processes, from a specific vibrational level in S_1 the molecules can either return back to the ground state S_0, by emitting fluorescence after vibrational relaxation (VR) steps, or reach the first excited triplet state T_1 by intersystem crossing (IC). From this first excited triplet state T_1, molecules vibrationally relax and radiatively return to the ground electronic state S_0 by emitting phosphorescence. Phosphorescence results thus from the radiative deexcitation of the triplet excited state and it is characterized by a lower intensity and longer lifetime compared with fluorescence.

Fluorescence and phosphorescence properties of liquid acetone under 266 nm wavelength excitation have been studied by Tran et al. (2006), who demonstrated that the fluorescence intensity of liquid acetone was not pressure dependent in the range [1 – 15 bars]. In addition, whatever the pressure value, Tran et al. observed a phosphorescence lifetime around 1 µs, much smaller than in the vapor phase. Phosphorescence properties of liquid and vapor acetone excited at 308 nm have been studied at atmospheric pressure by Charogiannis and Beyrau (2013). They observed that the phosphorescence intensity of vapor acetone in nitrogen gas was slightly decreasing with time and was much lower than the fluorescence intensity. The pressure dependence of acetone vapor fluorescence following excitation at 248, 266 and 308 nm in the pressure range from 5×10^4 to 1.6×10^6 Pa has been investigated in (Thurber and Hanson, 1999). It was observed that the fluorescence intensity was gradually increasing with pressure at all excitation wavelengths, till a high pressure limit; this limit was more quickly reached at the highest investigated wavelength, namely 308 nm. A simplified yield model for acetone fluorescence as a function of pressure, temperature and excitation wavelength was also presented, and the fluorescence intensity was given by:

$$S_f = n_{op}\frac{E\,\lambda}{h\,c}V_c\,n_{ac}\,\sigma\,\varphi \qquad (1)$$

where S_f is the fluorescence intensity, n_{op} is the collection optics efficiency, E the laser fluence [J/m²], $h\,c/\lambda$ [J] the energy of a photon at the excitation wavelength λ, V_c [m^3] the collection volume, n_{ac} [m^{-3}] the number density of acetone, $\sigma(\lambda,T)$ [m^2] the absorption cross section depending on the excitation wavelength and the temperature T. $\varphi(\lambda,T,p,c_i)$ is the fluorescence quantum yield depending on the excitation wavelength λ, the temperature T, the pressure p and the molar concentration ci of the quenching species :

$$\varphi = \frac{K_f}{K_f + K_{coll} + K_{NR,1}} + \sum_{i=2}^{N-1}\left(\frac{K_f}{K_f + K_{coll} + K_{NR,i}}\prod_{j=1}^{i-1}\left(\frac{K_{coll}}{K_f + K_{coll} + K_{NR,j}}\right)\right) + \frac{K_f}{K_f + K_{NR,N}}\prod_{j=1}^{N-1}\left(\frac{K_{coll}}{K_f + K_{coll} + K_{NR,j}}\right) \qquad (2)$$

In Eq. (2), K_f is the fluorescence rate assumed constant, K_{coll} the collision rate, K_{NR} the non-radiative rate and N the number of vibrational levels. The dependence of the fluorescence yield φ vs pressure is displayed in Fig.2. Details on this model and an algorithm for φ calculation can be found in (Thurber and Hanson 1999).

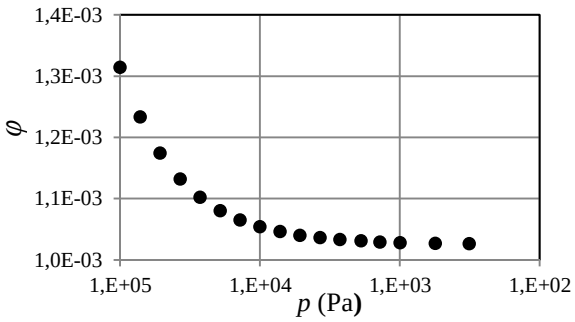

Fig. 2 Fluorescence quantum yield vs pressure of acetone argon mixture. T = 293 K, λ=266nm and acetone molar concentration c=10.4%

In the present paper, the influence of pressure on the acetone vapor luminescence inside argon gas is investigated with the aim of using acetone as a tracer for analyzing gas flows in the slip flow regime by molecular tagging velocimetry. After a presentation of the experimental setup (section 2), acetone phosphorescence decay with time is discussed (section 3.1). Then, the pressure dependence of acetone luminescence is studied in the range [$10^2 - 10^5$ Pa] (section 3.2). Next, as the diffusion phenomenon becomes significant at lower pressures, we propose (section 3.3) a preliminary study of the diffusion effects as well as an estimation of the diffusion coefficient at specific experimental conditions. Finally, implications for molecular tagging velocimetry and concluding remarks are presented (sections 4 and 5).

2. Experimental setup

A global view of the experimental setup used in this study is presented in Fig. 4. The excitation is made by a frequency-quadrupled dual frame Nd: YAG laser with a wavelength of 266 nm. The laser generates 4 ns pulses, and provides a beam with a maximum energy of 30 mJ, reduced to 0.17 mJ with an integrated attenuator. The initial laser beam has a 6 mm diameter, and it is focused with a diaphragm and a focusing lens down to a diameter of 35 µm.

Fluorescence and phosphorescence signals are collected by a 12-bit progressive scan camera with a CCD detector coupled to a 25 mm intensified relay optics (IRO). The 1376×1040 pixels CCD sensor has an operating frequency of 10 frames per second. The optics of the camera is a 105 mm Micro Nikkor lense.

The gas circuit is schematized in Fig. 3. A small reservoir has been added between valves V1 and V2 to create a capacitance for smoothing possible pressure fluctuations. Argon-acetone mixture is generated by bubbling argon in a thermally regulated liquid acetone bath. This bath is equipped with a thermocouple and a pressure sensor.

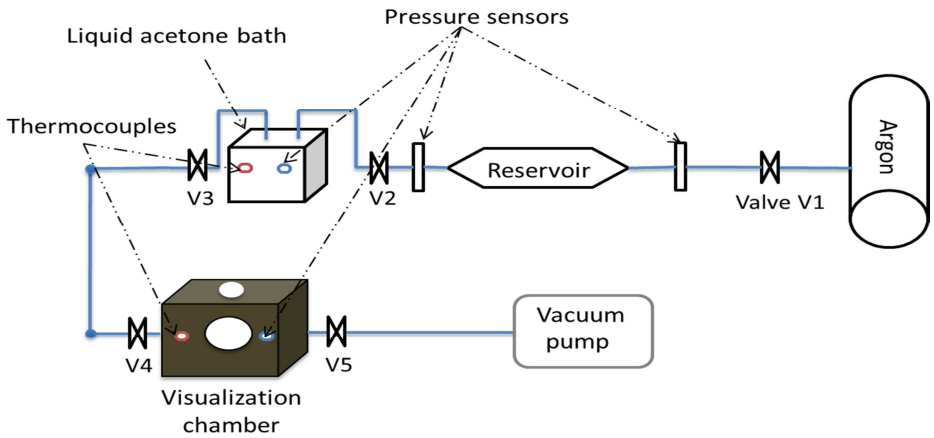

Fig. 3 Gas circuit.

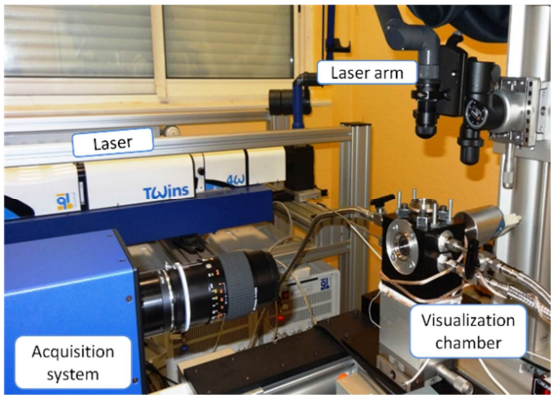

Fig. 4 Global view of the experimental setup.

The visualization chamber is equipped with two 19 mm diameter windows: the upper one for the laser beam access and the frontal one for the camera access perpendicularly to the laser axis. A thermocouple and an Inficon® capacitive pressure gauge are used to measure operating conditions in the visualization chamber. The pressure is adjusted by a vacuum pump. All experiments are performed at room temperature and with gas at rest, valves V4 and V5 being closed during the acquisition. The acquisition of the luminescent signal is performed with the on-chip integration method by selecting a CCD exposure time long enough to capture a series of laser pulses. Details on this technique, which dramatically increases the signal to noise ratio, can be found in (Samouda et al., 2013).

3. Results and discusion

3.1 Phosphorescence decay

The phosphorescent signal of acetone gas in argon is collected from t = 0.75 to 1200 µs at pressure $p = 9.9\times10^4$ Pa and temperature $T = 294$ K, with an IRO gate t_g = 500 ns. This means that the signal is collected between t and $t + t_g$. Two IRO gains, 90 and 100 %, are used with an appropriate correction allowing comparison of the intensity measured with both gains. The camera is opened during 10 s, which allows integrating the signal relative to 100 laser shots on a single image. 50 integrated images are then collected in the same conditions and averaged. The final image is consequently obtained from the signal of 100 × 50 = 5000 laser shots. In order to increase the level of the signal, 4×4 binning has been activated and leads to an area of 344×260 pixels, among which 40×100 pixels covers the 3.65×9.1 mm^2 region of interest.

The signal intensity S shown in Fig. 5 represents the averaged value, along the beam axis, of the maximal signal intensity taken in each cross-section of the beam. S is normalized by its value S_0 measured at $t = 0.75$ µs. The operating conditions are close to ambient conditions with a molar concentration of acetone $c = 9.8$ %. It is observed that the phosphorescence signal is rapidly decreasing with time, closely following a power law, as shown in Fig. 5. No exploitable signal can be collected after 1200 µs.

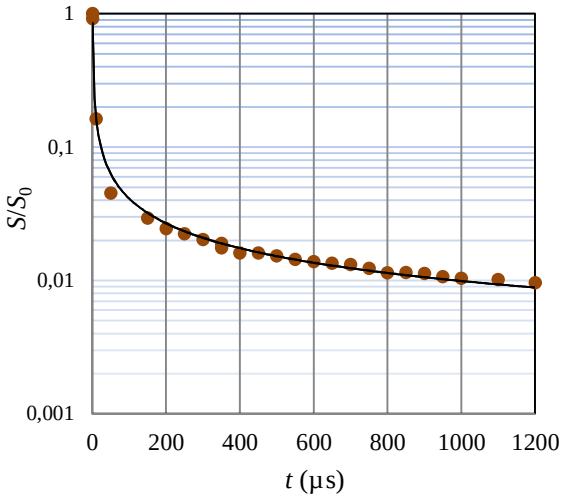

Fig. 5 Decay with time of acetone phosphorescence in argon: phosphorescence intensity S is normalized with its value S_0 at $t = 0.75$ µs. $T = 294$ K, $p = 9.9\times10^4$ Pa and $c = 9.8$%.

These experiments clearly demonstrate that the acetone phosphorescence lifetime can be much higher than the value of 200 µs usually claimed in the literature (Kaskan and Duncan 1950; Groh et al., 1953; Gandini and Kutschke 1968).

3.2 Pressure dependence of luminescence

Fluorescence and phosphorescence properties of acetone vapor in argon are investigated in the pressure range from 10^2 to 10^5 Pa and with a temperature of 294 K. The visualization chamber is filled in with acetone-argon mixture in three steps. First, vacuum is generated

inside by opening valve V5 and activating the vacuum pump during 30 minutes. Second, a flow of acetone-argon mixture is generated through the gas circuit with valves V1, V2, V3, V4 and V5 (Fig. 3) opened, and the visualization chamber is downstream open to outside. In the third step all valves are closed and the visualization chamber is connected again to the vacuum pump. Then, to ensure thermal stability the pressure is gradually reduced by pumping and the acquisition is started 30 min after reaching the desired pressure. The IRO gate is set to the shortest allowed value, namely 100 ns, for fluorescence and to 500 ns for phosphorescence acquisition.

For fluorescence tests, the IRO gain is set to 55 % and the IRO is opened 90 ns before the laser shot to avoid adding significant phosphorescence to fluorescence signal. The effective signal is then measured from $t = 0$ to $t = 10$ ns, which covers all the fluorescence duration. The fluorescence intensity S_f normalized by its value S_{f0} measured at atmospheric pressure is displayed in Fig. 6 as a function of pressure.

Fluorescence intensity is continuously decreasing with pressure, following a power law, i.e. a straight line in the log-log plot of Fig. 6. At the lowest investigated pressure, 1.4×10^2 Pa, the fluorescence intensity is 200 times lower than at atmospheric pressure. This lowest intensity is, however, still clearly detectible and usable for MTV experiments. The experimental data are compared to a very simple law (dashed line with slope −1 in Fig. 6) assuming that fluorescence is proportional to the number of acetone molecules, i.e. proportional to the pressure for a given value of the concentration c of acetone in argon. This simple assumption is improved by Eq. (1) taking into account the fluorescence quantum yield dependence with pressure (see Fig. 2), which leads to a slight modification of $S(p)$. The normalized fluorescence intensity predicted by Eq. (1), however, remains a function of pressure close to a power law (see straight plain line in Fig. 6). Although the experiment reveals a power law for $S(p)$, experimental data are not in total agreement with the model proposed by Thurber and Hanson (1999) in Eq. (1), which predicts a 5 times faster decrease of fluorescence intensity with pressure than experimentally observed. This deviation with Eq. (1) requires further analysis.

The early phosphorescence signal is then investigated at a delay of 100 ns using two different gains, 90 % and 100 %. The phosphorescence intensity S_p normalized by its value S_{p0} at atmospheric pressure is also plotted as a function of pressure in Fig. 6, and compared to the normalized fluorescence intensity. In the same temperature and concentration conditions, the ratio S_{f0} / S_{p0} = 640, which shows a dramatic decrease of the luminescent intensity when passing from fluorescence to phosphorescence.

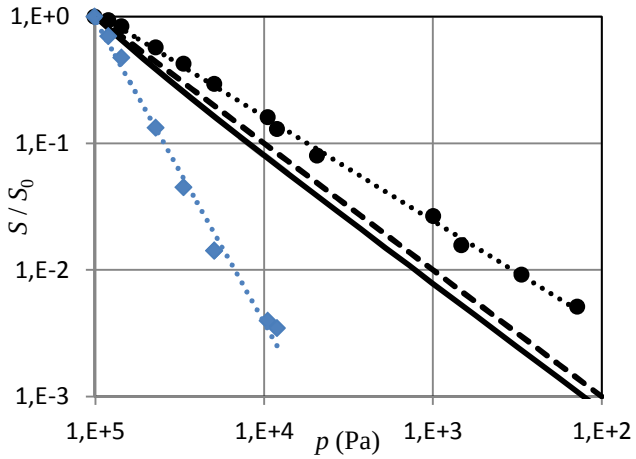

Fig. 6 (♦) Experimental early phosphorescence intensity S_p normalized by its value S_{p0} at atmospheric pressure (100 ns < t < 600 ns); (●) experimental fluorescence intensity S_f normalized by its value S_{f0} at atmospheric pressure (0 < t < 10 ns) compared with (**—**) the model from Eq. (1). T = 294 K and c = 10.4 %.

Both fluorescence and phosphorescence decrease as a power law with pressure, the power coefficient being roughly three times higher for phosphorescence than for fluorescence. Below 8×10^3 Pa, the phosphorescence signal is not exploitable any longer with the acquisition parameters listed above. However, increasing the gate to 1000 ns, the gain to 100 % , the number of averaged images from 50 to 100 and acetone mass concentration to 24.1 %, allows detecting an exploitable signal at t = 50 µs and $p = 2.2\times10^3$ Pa (Fig. 7).

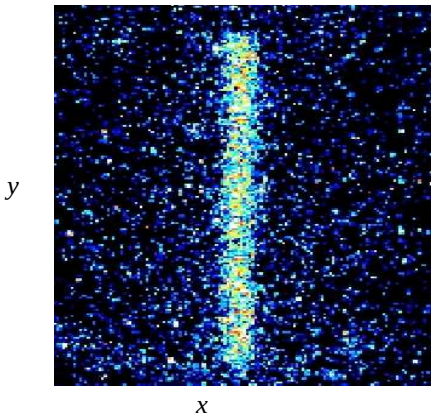

Fig. 7 Raw phosphorescence image. 50 µs < t < 51 µs, p = 2.2×10^3 Pa, T = 294.3 K and c = 24.1 %.

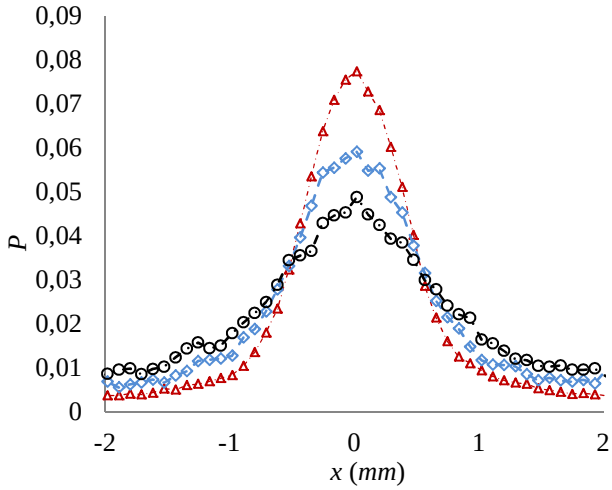

Fig. 8 Probability density function $P(x)$ of tagged molecules at t = 0.5 µs (Δ), t = 300 µs (◊) and t = 600 µs (o)., T = 292.3 K, p = 9.86×10^4 Pa and c = 25 %.

3.3 Diffusion effects

As expected and due to diffusion, it is observed that during the acquisition, the tagged region width in the direction x perpendicular to the laser beam axis y is increasing with time. The probability density function $P(x)$ of tagged molecules displayed in Fig. 8 is defined as:

$$P(x,t) = \int_{-H/2}^{H/2} \bar{S}(x,y,t)\mathrm{d}y \qquad (3)$$

with

$$\bar{S}(x,y,t) = \frac{S(x,y,t)}{\int_{-H/2}^{H/2}\int_{-W/2}^{W/2} S(x,y,t)\mathrm{d}x\mathrm{d}y} \qquad (4)$$

In these equations, $S(x,y)$ is the signal intensity, W and H are the width and the height of the region of interest, in the x- and y-directions, respectively.

The profile of $P(x)$ flattens as time increases, due to molecular diffusion of the tagged acetone molecules in the argon-acetone gas mixture.

It is assumed that the diffusion of tagged molecules, through the carrier gas at rest, is described by the equation

$$\frac{\partial P}{\partial t} = D\,\nabla^2 P - \alpha P \qquad (5)$$

$P(x,y,z,t)$ is the probability density associated with tagged molecules position within the channel region at time t, whereas D is the diffusion coefficient. The source term $-\alpha P$ describes the decay of tagged molecules as a result of fluorescence/phosphorescence, α being the time constant of the process. The source term can be eliminated by the following rescaling:

$$P(x,y,z,t) = \exp(-\alpha t)\,\bar{P}(x,y,z,t) \qquad (6)$$

where the new unknown $\bar{P}(x,y,z,t)$ obeys the equation:

$$\frac{\partial \bar{P}}{\partial t} = D\,\nabla^2 \bar{P} \qquad (7)$$

Since the tagged molecules displacements are small when compared with the visualization chamber width W, the x coordinate domain is considered unbounded. Accordingly, $\bar{P}$ (or P) is defined in the domain $\Omega = \{(x,y,z) \in \mathcal{R}^3 : -\infty < x < +\infty;\ -H/2 < y < H/2;\ -L/2 < z < L/2\}$.

Under the assumption that collisions with channel walls do not cause tagged molecules absorption by promoting deexcitation, the following boundary conditions can be assigned at walls:

$$\left.\frac{\partial \bar{P}}{\partial y} = 0\right|_{y=\pm\frac{H}{2}} \quad ; \quad \left.\frac{\partial \bar{P}}{\partial z} = 0\right|_{z=\pm\frac{L}{2}} \qquad (8)$$

The reduced probability density $\bar{P}_x = \iint \bar{P} dydz$ of the tagged molecules coordinate x obeys the one-dimensional diffusion equation:

$$\frac{\partial \overline{P_x}}{\partial t} = D \frac{\partial^2 \overline{P_x}}{\partial x^2} \qquad (9)$$

as a consequence of Eqs. (7,8). It is then easily shown that the variance $V(t)$ of the tagged molecules cordinate x evolves in time as:

$$V(t) = 2D\,t + V_0 \qquad (10)$$

This variance is used to describe the evolution of the tagged line width along the x-direction. It should be observed that, when the degree of gas rarefaction increases, the diffusion equation approximation requires the adoption of an effective diffusion coefficient which also takes into account gas-surface interaction (Dongari et al. 2009)

The measured time evolution of V is displayed in Fig. 9. The values of V deduced from experiments. As expected and according to Eq.10 V is linearly increasing with time.

The diffusion coefficient D can be also extracted from experimental data by linear fitting of V. From the data showed in Fig. (9), the value obtained at T = 292.3 K and $p = 9.86\times10^4$ Pa is $D = 4.75\times10^{-5}$ m² s^{-1} which is higher than the value of 8×10^{-6} m².s^{-1} measured for acetone-argon at T = 303 K and $p = 1\times10^5$ Pa by Kashirskaya et al. (2008). Although a direct comparison cannot be made between our study and the aforementioned one, because (i) the difference in operating conditions and (ii) the fact that the current diffusion coefficient concerns the acetone molecules diffusion in acetone-argon mixture, whereas the aforementioned value of D concerns the diffusion of acetone in argon. Moreover due to the very slow growth of the tagged region width (it increases from 1.634 mm at t = 0.5 µs to 2 mm at t = 900 µs, corresponding to an increase from 18 to 22 pixels), the camera resolution used in this study strongly increases the uncertainty in the diffusion coefficient estimation.

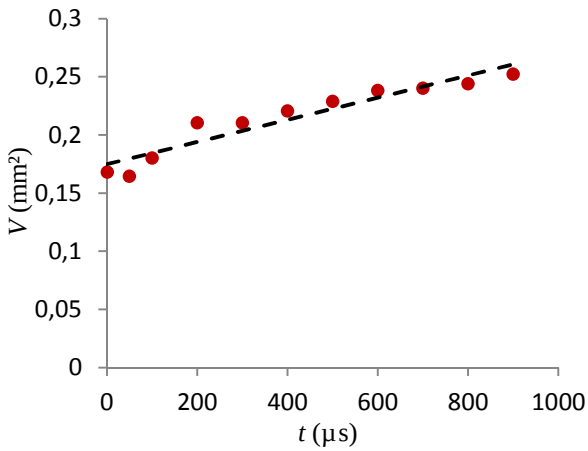

Fig. 9 Measured values of V vs t (●), (- -) linear fit

4. Implications for molecular tagging velocimetry

The long acetone phosphorescence lifetime observed in this study, around 1.2 ms, opens new possibilities to study slow flows. The use of a 1 ms delay and a camera resolution of 20 µm can allow measuring velocity profiles of argon flow in a channel of 1mm width at Reynolds numbers in the order of 10.

The increase of the luminescent region width over time observed in this study and due to the molecular diffusion of the tagged molecules can be described by the diffusion equation and the experimental analysis of enlargement of the tagged line can provide the value of the binary diffusion coefficient of acetone in acetone-argon mixture.

Despite the decrease of acetone fluorescence and phosphorescence intensities with pressure, it is however possible to use acetone as tracer for velocity measurement in rarefied regimes: for example, the phosphorescence signal observed at t = 50 µs and $p = 2.2\times10^3$ Pa (Fig. 8) allows analyzing argon flow in a 1 mm wide channel at a Knudsen number $Kn = 2.53\times10^{-3}$.

5. Conclusions

The pressure dependence of acetone vapor luminescence in argon, resulting from a UV excitation at a wavelength of 266 nm, has been experimentally investigated. The decay of acetone luminescence intensity with time at

atmospheric pressure shows that the phosphorescence lifetime is around 1200 µs, much higher than the 200 µs usually claimed in the literature (Kaskan and Duncan 1950; Groh et al., 1953;Gandini and Kutschke 1968). This discrepancy may be explained by the difference in the tagging and acquisition facilities between the previous and the present study.

Both fluorescence and phosphorescence signals are decreasing with pressure closely following a power law, with a slope three times higher in the case of phosphorescence. The fluorescence signal collected at the lowest investigated pressure, 1.4×10^2 Pa, is still clearly detectible and usable for MTV experiments. Improving the acquisition parameters and increasing the acetone concentration allow collecting exploitable phosphorescence signal at t = 50 µs and at pressures as low as p = 2.2×10^3 Pa, which corresponds to the slip flow regime in a 1 mm wide channel.

All measurements were performed in the visualization chamber with a gas at rest. This improves the simplicity of the gas circuit and facilitates the control of operating conditions. However, the non-renewed acetone is subject to laser photolysis and this affects acetone reemission. For this reason, better results can reasonably be expected in the case of flow.

6. Acknowledgements

This research obtained financial support from the European Community's Seventh Framework Program (FP7/2007-2013) under grant agreement no 215504, from the Fédération de Recherche Fermat, FR 3089, and from the Project 30176ZE of the PHC GALILEE 2014 Program.

7. References

Basu, R., Naguib, A. M., & Koochesfahani, M. M. (2010). Feasibility study of whole-field pressure measurements in gas flows: molecular tagging manometry. Experiments in Fluids, 49(1), 67-75.

Brune, F., Cid, E., Bartoli, A., Bouche, E., Risso, F., & Roig, V. (2013). Image registration algorithm for molecular tagging velocimetry applied to unsteady flow in Hele-Shaw cell. Experimental Thermal and Fluid Science, 44, 897-904.

Charogiannis, A., & Beyrau, F. (2012). Investigation of laser induced phosphorescence properties of acetone. 16th Int Symp on Applications of Laser Techniques to Fluid Mechanics. Lisbon, Portugal.

Charogiannis, A., & Beyrau, F. (2013). Laser induced phosphorescence imaging for the investigation of evaporating liquid flows. Experiments in Fluids, 54(5), 1-15.

Colin, S. (2012). A critical review on convective heat transfer. Journal of Heat Transfer, 134 (2), 020908.

Colin, S., Lalonde, P., & Caen, R. (2004). Validation of a second-order slip flow model in rectangular microchannels. Heat Transfer Engineering, 25(3), 23–30.

Dongari, N., Sharma, A., & Durst, F. (2009). Pressure-driven diffusive gas flows in micro-channels: from the Knudsen to the continuum regimes. Microfluidics and Nanofluidics, 6(5), 679-692.

ElBaz, A., & Pitz, R. (2012). N2O molecular tagging velocimetry. Applied Physics B, 106, 961–969.

Gandini, A., & Kutschke, K. O. (1968). The Primary Process in the Photolysis of Hexafluoroacetone Vapour. II. The Fluoresence and Phosphorescence. Proceedings of the Royal Society of London. Series A. Mathematical and Physical Sciences , 136(1487), 511-528.

Garbe, C. S., Roetmann, K., Beushausen, V., & Jahne, B. (2008). An optical flow MTV based technique for measuring microfluidic flow in the presence of diffusion and Taylor dispersion. Experiments in Fluids, 44, 439–450.

Groh, H. J., Luckey, G. W., & Noyes, W. A. (1953). The Mechanism of Acetone Vapor Fluorescence. The Journal of Chemical Physics 21(1): 115-118.

Kashirskaya, O. A., Lotkhov, V., & Dil'man, V. (2008). The Determination of Molecular Diffusion Coefficients by the Barometric Method. Russian Journal of Physical Chemistry, 82(7), 1225–1228.

Kaskan, W., & Duncan, A. B. (1950). Mean Lifetime of the Fluorescence of Acetone and Biacetyl Vapors. The Journal of Chemical Physics 18(4): 427-431.

Koochesfahani, M. (1999). Molecular Tagging Velocimetry (MTV): Progress and Applications. 30th AIAA Fluid Dynamics Conference. Norfolk.

Morini, G. L., Yang, Y., Chalabi, H., & Lorenzini, M. (2011). A critical review of the measurement techniques for the analysis of gas microflows through microchannels . Experimental Thermal and Fluid Science, 35(6), 849-865.

Samouda, F., Colin, S., Barrot, C., Baldas, L., & Brandner, J. J. (2013). Micro molecular tagging velocimetry for analysis of gas flows in mini and micro systems. Microsystem Technologies.

Sinton, D. (2004). Microscale flow visualization. Microfluid Nanofluid, 1, 2:21.

Thurber, M., & Hanson, R. (1999). Pressure and composition dependences of acetone laser-induced fluorescence with excitation at 248, 266, and 308 nm. Applied physics B(69), 229-240.

Tran, T., Kochar, Y., & Seitzman, J. (2006). Measurements of acetone fluorescence and phosphorescence at high pressures and temperatures. 44th aerospace sciences meeting and exhibit. Nevada.

Zhang, W.-M., Meng, G., & Wei, X. (2012). A review on slip models for gas microflows. Microfluidics and Nanofluidics, 13(6), 845-882.